UC San Diego

UC San Diego Previously Published Works

Title

Diagnosis, Prognosis, and Maintenance Decision Making for Civil Infrastructure: Bayesian Data Analytics and Machine Learning

Permalink

https://escholarship.org/uc/item/75z8q68h

ISBN

9783030817152

Authors

Vega, Manuel A
Hu, Zhen
Yang, Yichao
et al.

Publication Date

2022

DOI

10.1007/978-3-030-81716-9_3

Peer reviewed

eScholarship.org Powered by the California Digital Library
University of California

Diagnosis, Prognosis, and Maintenance Decision-Making for Civil Infrastructure: Bayesian Data Analytics and Machine Learning

Manuel A. Vega[1], Zhen Hu[2], Yichao Yang[3], Mayank Chadha[4], and Michael D. Todd[5]

[1,3,4,5] University of California San Diego, La Jolla, CA 92093, USA
[2] University of Michigan-Dearborn, Dearborn, MI 48128, USA
[1]mvegaloo@eng.ucsd.edu, [2]zhennhu@umich.edu, [3]yiy018@eng.ucsd.edu,
[4]machadha@eng.ucsd.edu, [5]mdtodd@eng.ucsd.edu

Abstract. Due to the aging of civil infrastructure and the associated economic impact, there is an increasing need to continuously monitor structural and non-structural components for system life cycle management, including maintenance prioritization. For complex infrastructure, this monitoring process involves different types of data sources collected at different time scales and resolutions, including but not limited to abstracted rating data from human inspections, historical failure record data, uncertain cost data, high-fidelity physics-based simulation data, and online high-resolution structural health monitoring (SHM) data. The heterogeneity of the data sources poses challenges to implementing a diagnostic/prognostic framework for decision-making for life cycle actions such as maintenance. Using quoin blocks components of a miter gate as an example, this chapter presents a holistic Bayesian data analytics and machine learning (ML) framework to demonstrate how to integrate various data sources using Bayesian and ML methods for effective SHM, and Prognostics and Health Management (PHM). In particular, this chapter discusses how Bayesian data analytics and ML methods can be applied to (1) diagnosis of bearing loss-of-contact degradation in quoin blocks; (2) optimized sensor placement for SHM on the gate; (3) fusion of various data sources for effective PHM; and (4) deciding maintenance-strategies by considering the behavioral aspect of human decision-making under uncertainty.

Keywords: Bayesian methods; uncertainty quantification; FE model; surrogate model; damage estimation; remaining useful life prediction; decision-theory

1 Introduction

Advances in sensing technologies, accelerated by the "internet-of-things," have allowed collection of large amounts of data about our civil infrastructure, which includes complex transportation networks both over land and through our inland waterway navigation corridors. Among the most important reasons for this data collection are damage/state diagnostics and predictions of future state performance. Such assessments can lead to improved life-cycle management of civil infrastructure systems, which is critical

to keep these systems continuously operational under increasingly constrained budgets. Figure 1 shows an overview of the association between diagnosis, prognosis, and maintenance decision making for civil infrastructure; more detail can be found in [1]. In a general sense, Figure 1 shows the fundamental workflow of a "digital twin" for structural asset life cycle diagnosis and prognosis.

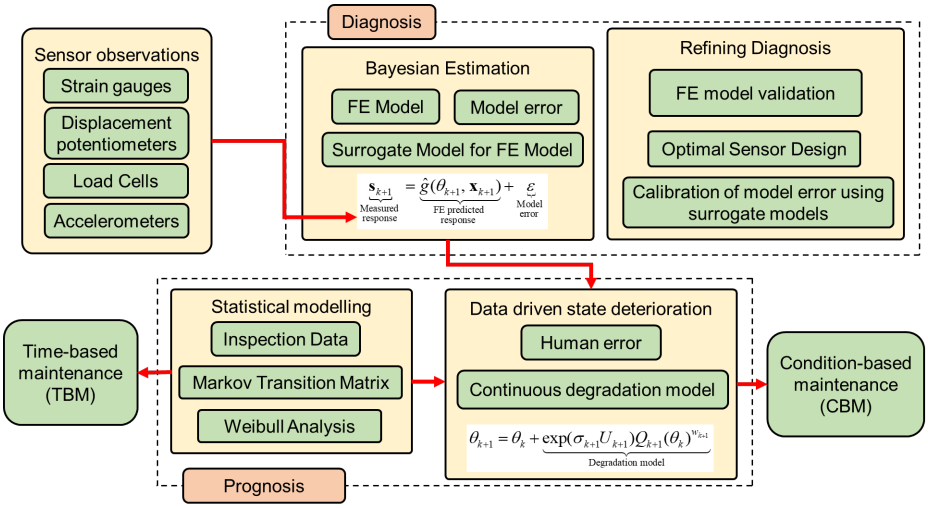

Fig. 1. Diagnosis, Prognosis, and Maintenance Decision Making Framework for Civil Infrastructure

For damage diagnosis, engineers can rely on supervised learning algorithms when sufficient life-cycle data is available [2–4]. On the other hand, when life-cycle data is limited, engineers typically rely on physics-based modeling (such as finite element (FE) models) and model updating techniques to estimate the unknown parameters required to infer the current state of the system as indicated in Fig. 1.

Prognostics and Health Management (PHM) is the notion of augmenting current structural state diagnostic information gleaned by inspections or SHM to make predictions of the future state and reliability of the system based on degradation models or historic degradation/failure data [5]. When such prior data is available (not very common in the civil infrastructure domain), a data-driven degradation model is possible, but more commonly physics-based approaches [6,7] or empirical approaches to build the model [8–10] are required.

Additionally, PHM uses its prediction capabilities to inform life cycle management, which targets optimization of a desired system performance criterion (e.g., cost, availability, reliability, etc.). For life-cycle management, maintenance approaches can be roughly classified into two categories, namely time-based maintenance (TBM) and condition-based maintenance (CBM). This term is closely related to condition monitoring (CM), which usually refers to implementation of state diagnostics applied to rotating machinery [11]. When applied to civil and aerospace systems, CM is referred to as SHM, so these terms are used interchangeably in a general sense. When information from an SHM (equivalent, a CM) process is used to trigger maintenance decisions, a

CBM decision policy arises. TBM and CBM approaches have been benefited by advances in various fields such as data analytics, machine learning, computational mechanics, Bayesian statistics, and reliability engineering.

As stated before, diagnostic and prognostic approaches are either physics-based (e.g. FE model updating) [12–14] or data-driven [15–18]. For some engineering systems, hybrid approaches that combine the physics-based approach with data-driven approach to improve the CBM predictive capabilities are useful. However, the study of hybrid approaches [19,20] has been very limited, and even more limited for large civil infrastructure. Other limitations that occur, for example, are that the monitoring process sometimes involves different types of data sources collected at different time scales and resolutions, such as abstracted rating data from human inspections, historical failure record data, uncertain cost data, high-fidelity physics-based simulation data, and online high-resolution structural health monitoring (SHM) data. The heterogeneity of the data sources poses challenges to the diagnostic/prognostic implementation of decision-making for maintenance.

This chapter presents a holistic framework for diagnosis, prognosis, and maintenance decision making for civil infrastructure using Bayesian data analytics and machine learning methods. It combines a physics-based approach for diagnosis with data-driven approaches using various data sources for prognostics. In summary, this chapter discusses how to: (1) fuse various data sources using Bayesian methods; (2) perform damage diagnostics and prognosis using Bayesian data analysis and machine learning; (3) optimize maintenance strategies; and (4) apply these concepts to a real-world problem using a miter gate example, drawn from a navigation lock system used in the inland waterways navigation corridor.

2 Summary of data sources

2.1 Physics-based simulation data

For civil systems, the approach is usually carried out by using a physics-based model (e.g. finite element (FE) model) of the structure [2–4]. It is fundamentally an inverse problem because the system parameters are estimated from measured response quantities. Generally, a physics-based model is a “forward” problem where the system responses (e.g., FE output response) are predicted as a function of the (known) system parameters (e.g., FE inputs). Synthetic system parameters may be used to obtain the FE system response, whose responses can be compared to the “true” system as shown in Figure 2.

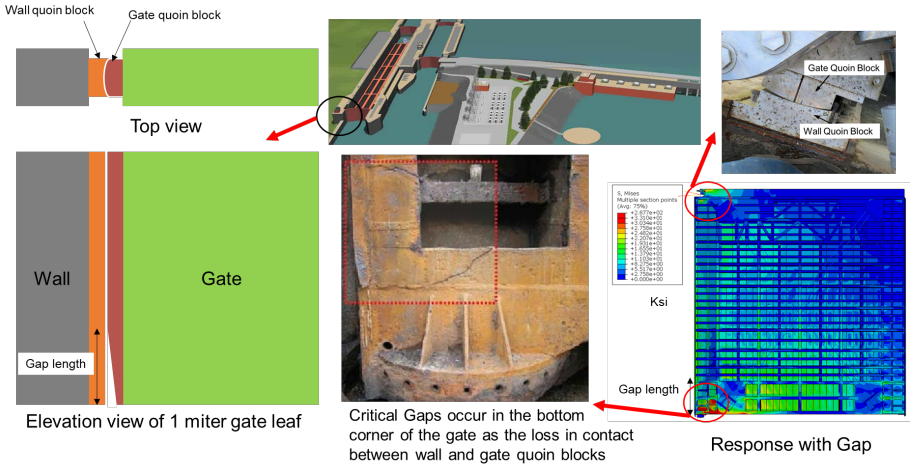

Fig. 2. FEM modelling of a leaf of a miter gate including gap length deterioration

2.2 Inspection data

Regular condition assessments are conducted in critical structures such as bridges and offshore structures. These assessments are obtained from an inspection process, which can be part of a periodic or non-periodic inspection policy. One may reasonably hypothesize that these inspections should reflect a deterioration state. These states can be in a continuous or discrete form, e.g., an inspection assignment of A, B, C, D, F, CF, such as is utilized for hydraulic structures owned by the U.S. Army Corps of Engineers (USACE). Inspections can be performed by inspectors, drones [21], or even robots [22]. The resulting data format is usually highly abstracted in the format of ratings as mentioned above.

In [23], the failure condition in critical components is estimated using a transition matrix built from the discrete inspection ratings. The following is an example of a transition matrix built from the reported 6 damage ratings:

$$\mathbf{P}_{\text{Report}} = P\left(\mathbf{X}_{t+1}^{R} \middle| \mathbf{X}_{t}^{R}\right) = \begin{bmatrix} P\left(A_{t+1}^{R} \middle| A_{t}^{R}\right) & \cdots & P\left(CF_{t+1}^{R} \middle| A_{t}^{R}\right) \\ \vdots & \ddots & \vdots \\ P\left(A_{t+1}^{R} \middle| CF_{t}^{R}\right) & \cdots & P\left(CF_{t+1}^{R} \middle| CF_{t}^{R}\right) \end{bmatrix}, \forall i, j = 1, \cdots, 6, \quad (1)$$

where $P(\cdot)$ is a probability operator, $\mathbf{X}_{t}^{R} = [A_{t}^{R}, B_{t}^{R}, C_{t}^{R}, D_{t}^{R}, F_{t}^{R}, CF_{t}^{R}]$ are the damage ratings at time step t, and "$|$" is a conditional operator.

The above transition matrix obtained from inspection data can be used to estimate the possible condition (and failure condition) after n time steps as follows:

$$P(\mathbf{X}_{n+k}^{R}) = P(\mathbf{X}_{k}^{R}) \cdot \mathbf{P}_{\text{Report}}^{n}, \quad (2)$$

where $P(\mathbf{X}_k^R)=[P\left(X_{1,k}^R\right), P\left(X_{2,k}^R\right), P\left(X_{3,k}^R\right), P\left(X_{4,k}^R\right), P\left(X_{5,k}^R\right), P\left(X_{6,k}^R\right)]$ are the condition probabilities at the current time or initial time (i.e. k=0) where $X_{1,k}^R$ and $X_{6,k}^R$ represents A_k^R and CF_k^R, respectively. The condition CF represents the complete failure condition. $\mathbf{P}_{\text{Report}}$ is the transition matrix built from the discrete ratings, and $P(\mathbf{X}_{n+k}^R)$ are the condition probabilities at n time steps in the future. The current time $P(\mathbf{X}_k^R)$ may be either obtained from current inspections or using SHM data.

2.3 Human errors

Human error can greatly affect the reliability of the inspection assessment. For example, human psychology influences inspectors to make conservative or nonconservative assessment that can greatly influence maintenance decisions. Benchmark data may be available to account for the accuracy of the assessment given the inspector qualification, training, and certification [24]. A human observation error matrix can be obtained/estimated as follows to probabilistically measure the human error

$$\mathbf{P}_{\text{human}}=\begin{bmatrix} P_{11}^h & P_{12}^h & \cdots & P_{16}^h \\ P_{21}^h & P_{22}^h & \cdots & P_{26}^h \\ \vdots & \vdots & \ddots & \vdots \\ P_{61}^h & P_{62}^h & \cdots & P_{66}^h \end{bmatrix}=\begin{bmatrix} P\left(A_t^R \middle| A_t^{tr}\right) & P\left(A_t^R \middle| B_t^{tr}\right) & \cdots & P\left(A_t^R \middle| CF_t^{tr}\right) \\ P\left(B_t^R \middle| A_t^{tr}\right) & P\left(B_t^R \middle| B_t^{tr}\right) & \cdots & P\left(B_t^R \middle| CF_t^{tr}\right) \\ \vdots & \vdots & \ddots & \vdots \\ P\left(CF_t^R \middle| A_t^{tr}\right) & P\left(CF_t^R \middle| B_t^{tr}\right) & \cdots & P\left(CF_t^R \middle| CF_t^{tr}\right) \end{bmatrix}, \tag{3}$$

in which $P_{ik}^h=\Pr\{X_{i,t}^{obs} \mid X_{j,t}^{tr}\}$ is the probability that the reported OCA rating is k given that the true OCA rating is i.

An example of a conservative human error matrix is given as below

$$\mathbf{P}_{\text{human}}=\begin{bmatrix} 1 & 0 & 0 & 0 & 0 & 0 \\ 0.04 & 0.96 & 0 & 0 & 0 & 0 \\ 0 & 0.40 & 0.60 & 0 & 0 & 0 \\ 0 & 0.03 & 0.17 & 0.80 & 0 & 0 \\ 0 & 0 & 0 & 0.03 & 0.97 & 0 \\ 0 & 0 & 0 & 0 & 0.03 & 0.97 \end{bmatrix}. \tag{4}$$

The above $\mathbf{P}_{\text{human}}$ models the behavior of an inspector that regularly tends to assess a component to be in a better condition than reality. Accounting for $\mathbf{P}_{\text{human}}$ allows to estimate the $\mathbf{P}_{\text{true}}$ and $P(\mathbf{X}_k^{tr})$ from $\mathbf{P}_{\text{Report}}$ as will be discussed in Sec. 4.2. The terms $\mathbf{P}_{\text{true}}$ and $P(\mathbf{X}_k^{tr})$ are the true transition matrix and the true condition probabilities, respectively, at the current time.

2.4 SHM data

SHM data involves periodically sampled response measurements from spatially distributed sensors, extraction of damage-sensitive features from these measurements and damage diagnosis using these features with either an inverse-problem approach or a data-driven approach.

As stated earlier, SHM diagnostic capabilities can inform the current state of the structure. However, SHM data inevitably will contain noise due to a variety of stochastic influences, not the least of which result from environmental and operational variability. In this chapter, the sensor monitoring data (i.e., strain measurement data for the miter gate example) at time step t_i is defined as $\mathbf{s}_i = [s_{i1}, s_{i2}, \cdots, s_{iN_S}]$, where N_S is the number of sensors. Also, $\mathbf{s}_{1:n} \triangleq \{\mathbf{s}_1, \mathbf{s}_2, \cdots, \mathbf{s}_n\}$ defines the sensor measurements collected up to t_n.

Next, the following section will discuss how to utilize the above data sources for the damage diagnostics, prognostics, and maintenance planning using Bayesian data analytics and machine learning.

3 Damage diagnostics using Bayesian data analysis and machine learning

In this section, a summary of how to perform damage diagnostics using simulation data and SHM data based on machine learning and recursive Bayesian updating is presented.

3.1 Surrogate modelling for physics-based models using machine learning

For damage diagnosis with limited SHM data, inverse modelling via physics-based models such as finite element (FE) models have been used with data from SHM systems to estimate parameters that infer some form of damage state. A fast, efficient simulation of complex FE models is essential for appropriately fast damage diagnosis. Depending on the dimension space of the inputs and outputs of interest, different machine learning techniques can be chosen to build "cheap" yet accurate surrogate models of the physics-based FE model. Two of the commonly used techniques, artificial neural networks and Gaussian process regression, are briefly summarized as below.

Artificial Neural Network (ANN). ANNs are an attractive option for surrogate emulation of FE models. This type of supervised learning model works well with classification (for discrete classes) and regression (for continuous processes) problems. However, ANNs are effective when a large amount of data is available, and they are built to create point estimates rather than probabilistic estimates. Some researchers [25–28] have used Bayesian inference to estimate the ANN's weight and model parameters, which has been referred to as Bayesian Neural Networks (BNN). BNNs are good for high-dimensional spaces and better handle the issue of limited data availability.

Gaussian Process Regression (GP). GP (or Kriging) models are an attractive option for surrogate architectures because they are built to quantify the uncertainty in the estimations rather than simply point-based estimates, as most other supervised learning

models (e.g., ANNs, support vector machines) do. Several researchers use GP regression to build Bayesian prediction models for civil engineering structures [23,29]. A GP surrogate model, $\hat{\gamma}_j = \hat{g}_j(\mathbf{x})$ is defined as

$$\hat{\gamma}_j = \hat{g}_j(\mathbf{x}) = \mathbf{f}(\mathbf{x})^T \boldsymbol{\alpha} + Z(\mathbf{x}), \tag{5}$$

where $\boldsymbol{\alpha}$, $\mathbf{f}(\mathbf{x})^T$, and $Z(\mathbf{x}) \sim N(0, \sigma_{GP}^2 \rho(\bullet,\bullet))$ are the coefficients of the trend function, the trend function, and a stationary Gaussian process, respectively.

The stationary Gaussian process uses a correlation function $\rho(\bullet,\bullet)$ to quantify the correlation between responses at any two points as below

$$\rho(\mathbf{x},\mathbf{x}') = \exp\left\{-\sum_{l=1}^{N_V} \omega_l (x_l - x_l')^2\right\}, \tag{6}$$

where N_V is the number of variables, and $\boldsymbol{\omega} = (\omega_1,\ldots,\omega_{N_V})^T$ is the vector of roughness parameters.

Furthermore, the aforementioned GP hyper-parameters $\boldsymbol{\upsilon} = \left(\boldsymbol{\alpha}, \sigma_{GP}^2, \boldsymbol{\omega}\right)$ are estimated using the maximum likelihood estimation method. After the estimation of the hyper-parameters $\boldsymbol{\upsilon}$ for any given inputs $\mathbf{x}$, the GP prediction are given by

$$\hat{\gamma}_j = \hat{g}_j(\mathbf{x}) \sim N(\mu_j(\mathbf{x}), \sigma_j^2(\mathbf{x})), \forall j = 1, 2, \cdots, r, \tag{7}$$

where $\mu_j(\mathbf{x})$ and $\sigma_j^2(\mathbf{x})$ are the mean and variance of the prediction of γ_j, respectively, for the input $\mathbf{x}$.

In applications such as the miter gate presented in this chapter, the output space of the simulation or the sensors available (e.g., hundreds or thousands of nodes in the FE model) can be large. Also, it is known that sensors located close to each other may contain highly correlated information. Therefore, dimension reduction techniques are usually used in conjunction with GP models or ANNs to build surrogate models for the physics-based FE model. A commonly used technique is singular value decomposition (SVD). SVD is a linear algebra technique used to transform high-dimensional matrices into a reduced dimensional space preserving most of the original information. Fig. 3 presents a generalize procedure of surrogate modeling based on a GP model and dimension reduction methods for a model with inputs $\mathbf{x}$ and $\boldsymbol{\theta}$. Following that, Fig. 4 shows the prediction process using the trained kriging model for given FEM input parameters and features obtained from dimension reduction.

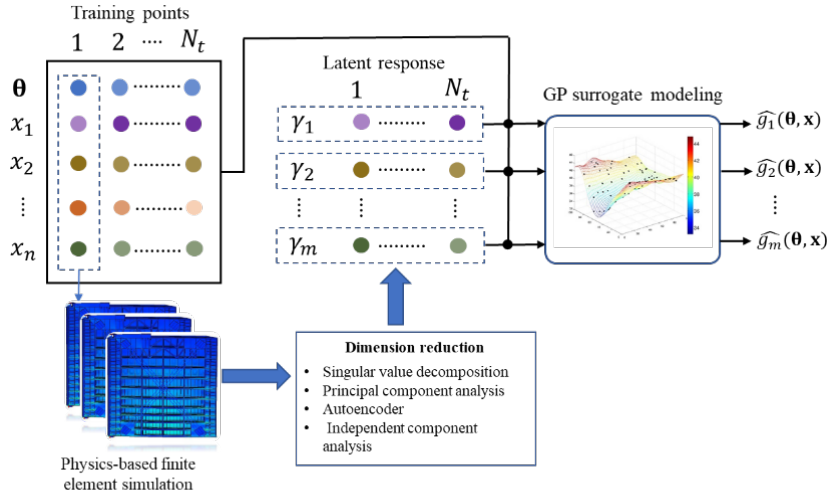

Fig. 3. Building Surrogate Model for FEM model using GP and dimension reduction

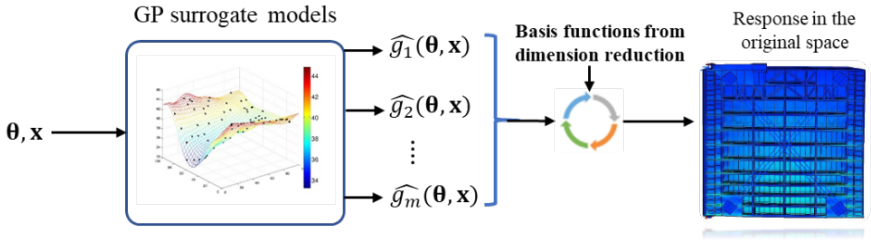

Fig. 4. Prediction using GP surrogate modeling and dimension reduction

The proposed framework explained in this work is based on a surrogate model using a Kriging model combined with SVD to develop a fast emulator of the FEM. Fig. 5 shows the testing accuracy obtained at 46 sensors installed in the Greenup miter gate at a particular point in time, which shows how close ML-based surrogate model emulates the original FE model.

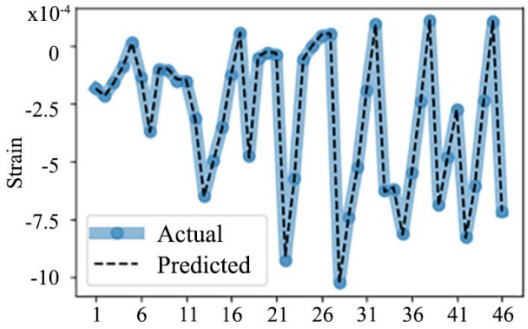

Fig. 5. Testing Accuracy of Kriging Model

3.2 Damage diagnostics using recursive Bayesian updating

Given the SHM data and a ML-based surrogate model of the physics-based FE model, damage diagnosis can be performed using Bayesian estimation of parameters, a_n, that directly relate to a damage mode (e.g., cracks, gap, thickness loss due to corrosion, etc. See Fig. 2 for examples). Bayesian estimation of this parameters can be performed based on the following state-space equation

$$\begin{aligned} &\text{State equation}: a_n = h(a_{n-1}) + \varepsilon_h, \\ &\text{Measurement equation}: \mathbf{s}_n = \hat{g}(a_n, \mathbf{x}_n) + \varepsilon_n, \end{aligned} \tag{8}$$

where $h(a_{n-1})$ is the state equation that describes the evolution of a_n over time, ε_h is the process noise, $\hat{g}(a_n, \mathbf{x}_n)$ is the ML surrogate model built in Sec. 3.1 where $\mathbf{x}_n$ represents the known/measurable input variables to the physics-based model (e.g. loads, geometry, material properties, etc.), and $\mathbf{s}_n$ are the observations from SHM system as discussed in Sec. 2.4.

Note that the state equation given in Eq. (8) may be unknown due to a lack of understanding of the damage evolution mechanism. In that situation, a random walk type equation can be used as the state equation with large process noise as discussed in [23]. Assume there are N_S strain sensors installed in a structure such as the miter gate and the damage parameter, a_n, to infer at time step t_n is the extent of the loss of bearing contacting (i.e. gap length). Then, the posterior probability density function of the gap length a_n at time step t_n conditioned on strain measurements $\mathbf{s}_{1:n}$ is estimated using Bayesian inference method recusively as follows

$$f(a_n \mid \mathbf{s}_{1:n}) = \frac{f(\mathbf{s}_n \mid a_n) f(a_n \mid \mathbf{s}_{1:n-1})}{\int f(\mathbf{s}_n \mid a_n) f(a_n \mid \mathbf{s}_{1:n-1}) da_n} \propto f(\mathbf{s}_n \mid a_n) f(a_n \mid \mathbf{s}_{1:n-1}), \tag{9}$$

which $f(a_n \mid \mathbf{s}_{1:n-1})$ is defined as follows

$$f(a_n \mid \mathbf{s}_{1:n-1}) = \int f(a_n \mid a_{n-1}) f(a_{n-1} \mid \mathbf{s}_{1:n-1}) da_{n-1}, \tag{10}$$

in which $f(\mathbf{s}_n \mid a_n)$ is the likelihood function, obtained from the measurement equation, of observing $\mathbf{s}_n$ for given a_n at time step t_n, and the term $f(a_n \mid a_{n-1})$ represents the probability distribution of a_n for a given a_{n-1} obtained using the state equation, which describes the damage evolution over time.

The recursive Bayesian updating of Eqs. (9) and (10) is analytically intractable. In practical application, various filtering methods, such as particle filtering [30], extended Kalman filter [31], and unscented Kalman filter [32], have been developed to approximate recursive updating process.

Fig. 6 presents an illustrative example of strain measurement data $\mathbf{s}_n$ of 10 sensors $(N_S = 10)$ over a certain time period of interest. After that, Fig. 7 shows the damage diagnostics results of gap length of miter gate (i.e., the gap damage in the miter gate as shown in Fig. 2) over time using recursive Bayesian updating and the ML-based surro-

gate models. It shows that the recursive Bayesian inference method can effectively perform damage diagnostics by fusing the information from physics-based simulation model and SHM data. More details of the integration of ML-based surrogate model and SHM observation data using Bayesian recursive updating for damage diagnostics are available in [23].

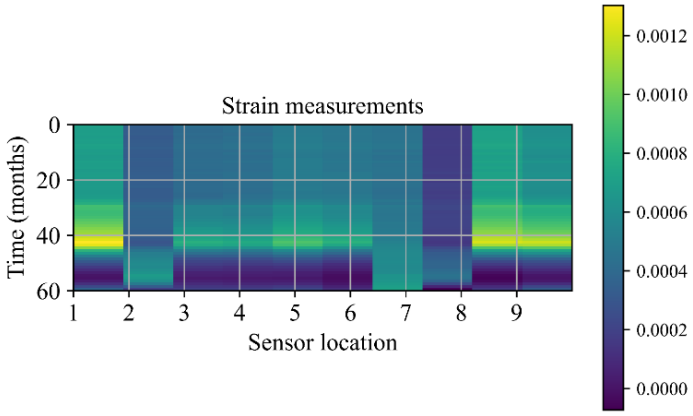

Fig. 6. Strain measurement from ten sensors over time

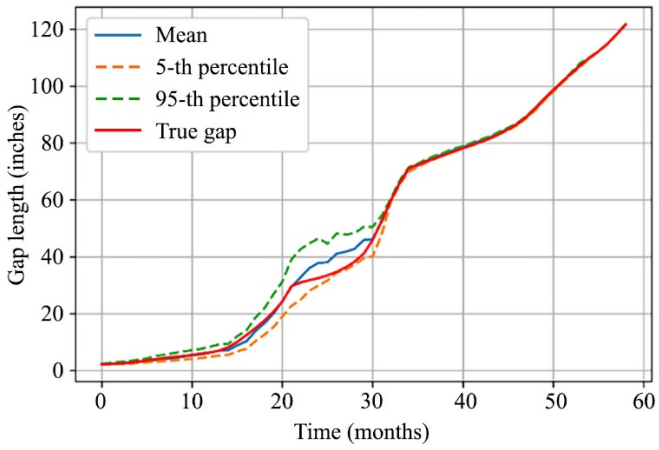

Fig. 7. Gap length diagnostics result using Bayesian method and ML surrogate model (note that Gap here refers to the damage mode shown in Fig. 2)

3.3 Sensor placement optimization for damage diagnostics using machine learning

Sensor placement optimization (SPO) plays a critical role in improving the effectiveness of the SHM system for damage diagnostics (see Eqs. (9) and (10)). Designing an optimal sensor network is very challenging in practice since the observations are not available in the design stage. In that case, the physics-based simulation model needs to

be employed to provide information on how to properly allocate the sensors. The physics-based model, moreover, is computationally very demanding. Machine learning techniques play a vital role in overcoming the challenges in SPO.

A SPO model can be generalized as follows

$$\begin{aligned} &\mathbf{d}^* = \arg\max_{\mathbf{d}\in\Omega_d} \{\Psi(\mathbf{d})\}, \\ &s.t.\ C(\mathbf{d}) \le C_e, \end{aligned} \tag{11}$$

where $\mathbf{d}$ is a sensor network design, Ω_d is the sensor design domain, $\Psi(\mathbf{d})$ is a cost function, $C(\mathbf{d})$ is the total cost of the sensor network, and C_e is the allowable budget.

The cost function $\Psi(\mathbf{d})$ may be formulated from different perspectives. For example, probability of detection [33], Bayes risk [34], and information gain [35] have been used as cost functions in sensor placement design optimization. Taking the information gain measured by the Kullback–Leibler (KL) divergence as an example, $\Psi(\mathbf{d})$ is formulated as

$$\Psi(\mathbf{d}) = \int_{\boldsymbol{\theta}} \int_{\mathbf{s}|\boldsymbol{\theta}} f_{\boldsymbol{\theta}}(\boldsymbol{\theta}) f_{\mathbf{s}|\boldsymbol{\theta},\mathbf{d}}(\mathbf{s}\,|\,\boldsymbol{\theta},\mathbf{d}) D_{KL}(\mathbf{d},\mathbf{s}) \mathbf{ds} \mathbf{d}\boldsymbol{\theta}, \tag{12}$$

where $D_{KL}(\mathbf{d},\mathbf{s}) = \int_{\boldsymbol{\theta}} f_{\boldsymbol{\theta}|\mathbf{s},\mathbf{d}}(\boldsymbol{\theta}\,|\,\mathbf{s},\mathbf{d}) \log\left[f_{\boldsymbol{\theta}|\mathbf{s},\mathbf{d}}(\boldsymbol{\theta}\,|\,\mathbf{s},\mathbf{d}) / f_{\boldsymbol{\theta}}(\boldsymbol{\theta}) \right] \mathbf{d}\boldsymbol{\theta}$ is the KL divergence (e.g. relative entropy) for given observations $\mathbf{s}$ and sensor placement design $\mathbf{d}$, which measures the difference (i.e., information gain) between the prior and posterior distributions of damage state variables $\boldsymbol{\theta}$.

Solving the sensor placement optimization model given in Eq. (11) is extremely challenging due to the high computational effort required in the repeated evaluations of Eq. (12). Bayesian data analytics and machine learning techniques are essential to overcome the challenge. First, ML models and Bayesian inference methods as discussed in Secs. 3.1 and 3.2 enables for the efficient estimation of the posterior distributions of the damage states variables. More importantly, ML-based optimization methods make it possible to solve the model given in Eq. (11) when a large number of sensors need to be allocated to a large civil infrastructure.

For example, when sensors need to be placed on the miter gate to detect the "gap" of the gate due to damage, the dimension of the design variables given in Eq. (11) will be very large. Assuming that 20 sensors need to be placed, the number of design variables will be 60, if the three-dimensional coordinates of each sensor are considered as design variables. In that case, directly solving the optimization model of Eq. (11) will be computationally prohibitive. Alternatively, a greedy-based framework can be employed to place the sensor one-by-one. In order to identify the optimal placement of the *i*-th sensor, the optimization model given in Eq. (11) is re-formulated as

$$\begin{aligned} &\mathbf{d}_i^* = \arg\max_{\mathbf{d}_i\in\Omega_d} \{\Psi(\mathbf{d}_i, \mathbf{d}_{1:i-1}^*)\}, \\ &s.t.\ C(\mathbf{d}) \le C_e \text{ and } \mathbf{d} = \{\mathbf{d}_i \cup \mathbf{d}_{1:i-1}^*\}, \end{aligned} \tag{13}$$

where $\mathbf{d}_{1:i-1}^*$ are the coordinates of the previous *i*-1 sensors and $\mathbf{d}_i$ are the coordinates of the *i*-th sensor.

Through the formulation of the model in Eq. (13), the dimension of the design variables is reduced to 3 in each iteration of the greedy optimization scheme. Even for the three-dimensional optimization model, the global optimization of Eq. (13) is still computationally challenging. Bayesian optimization method, which is also known as the efficient global optimization method, can be employed to efficiently solve the optimization model by leveraging the prediction capability of the Gaussian process model [36,37]. GP-based Bayesian optimization is a process of adaptively training a GP surrogate model for the objective function of an optimization model. In each iteration of the adaptive training of the GP, training data are identified as those design locations which have the highest probability of being the maximum/minimum design point. The key to the GP-based optimization is the definition of the expected improvement function (EIF)

$$\mathrm{EIF}(\mathbf{d}) = (\mu(\mathbf{d}) - \varphi^*)\Phi\left(\frac{\mu(\mathbf{d}) - \varphi^*}{\sigma(\mathbf{d})}\right) + \sigma(\mathbf{d})\phi\left(\frac{\mu(\mathbf{d}) - \varphi^*}{\sigma(\mathbf{d})}\right), \tag{14}$$

where $\phi(\cdot)$ and $\Phi(\cdot)$ are respectively the probability density function and cumulative distribution function of a standard normal random variable, φ^* is the current best values in the training dataset, $\mu(\mathbf{d})$ and $\sigma(\mathbf{d})$ are the mean and standard deviation of the GP surrogate model prediction.

By maximizing the EIF in Eq. (14), new training points may be identified to adaptively refine the GP surrogate model to approach the optimal value. Fig. 8 shows an illustrative example of Bayesian optimization using GP.

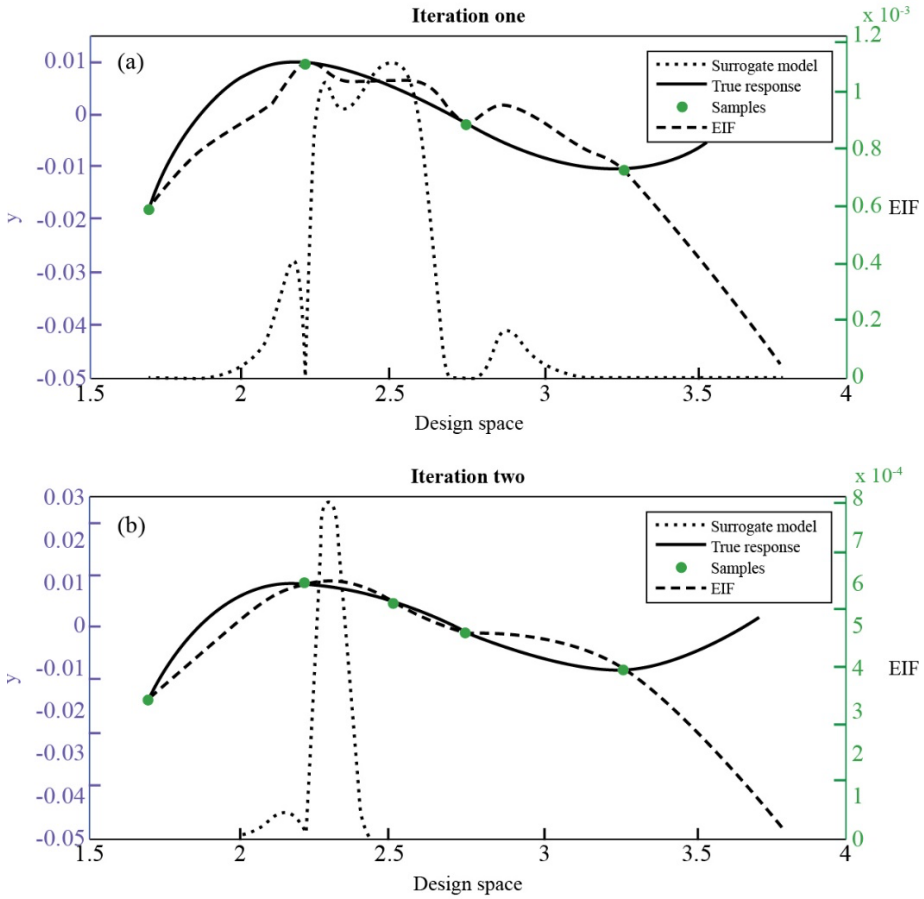

Fig. 8. An illustrative example of optimization using GP-based Bayesian optimization, (a) First iteration; (b) Second iteration.

As shown in Fig. 8, an initial GP surrogate model is trained first. Based on the trained GP surrogate model, the EIF values over the design space are computed as shown in Fig. 8(a). By maximizing the EIF, a new training point is identified, and the GP model is retrained in the second iteration as shown in Fig. 8(b). After a few of iterations, as illustrated in Fig. 9, the maximum point can be identified. These iterations show that the GP-based optimization needs very few evaluations of the objective function to identify the global optimization, which is much more efficient than the other global optimization algorithms, such as genetic algorithm, simulated annealing, and etc.

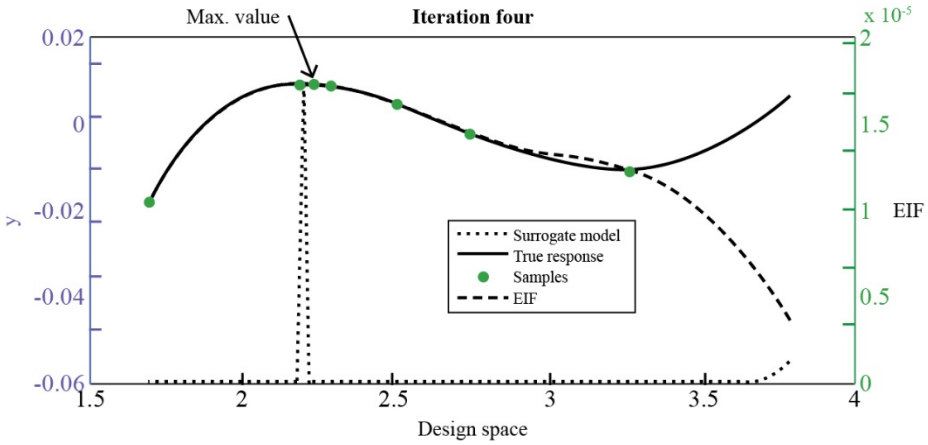

Fig. 9. An illustrative example of optimization using GP after converges.

The ML-based optimization method allows us to effectively allocate the optimal sensors and thereby increases the effectiveness of damage diagnostics as discussed in Sec. 3.2. Note that the greedy algorithm-based sensor placement design is an approximation of the original model. It may not find the "true" globally optimized sensor network. This limitation can also be mitigated using other ML methods, such as the reinforcement learning method, which may be better suited for dynamic optimization problems. Fig. 10 presents an example of sensor placement optimization results of miter gate obtained using the method presented in this section. More details are available in [38].

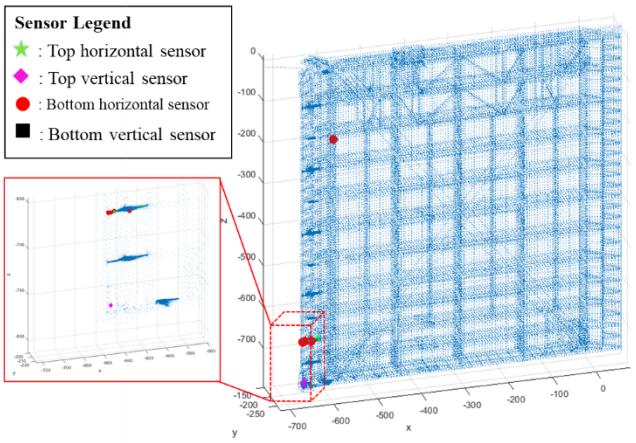

Fig. 10. An example of sensor placement optimization results using machine learning

4 Failure prognostics using Bayesian data analysis and machine learning

Failure prognostics is a process of predicting the end of life (EOL) of civil infrastructures to inform life-cycle management. Based on the state estimation from failure diagnostics as discussed in Sec. 3, the state of the system from the current time to a future time is obtained to predict the potential failure time or estimate the remaining useful life (RUL) of the system. Fig. 12 shows a schematic of how to use the predictions to calculate the EOL and RUL distributions.

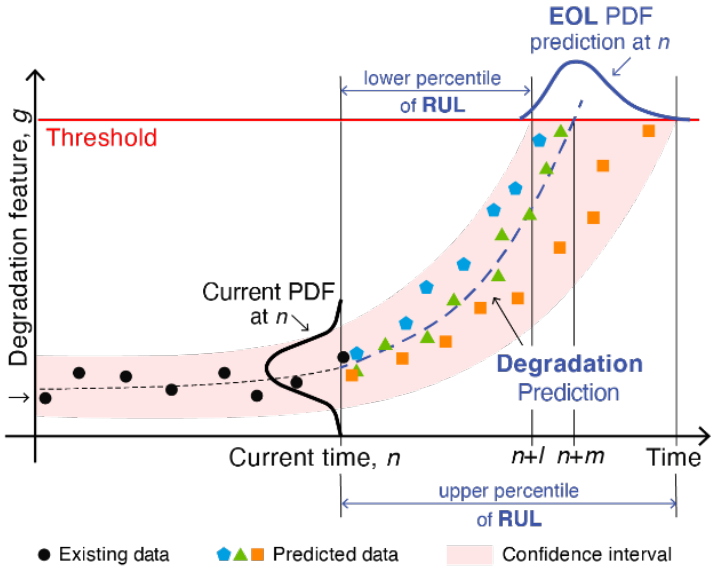

Fig. 11. RUL estimation based on failure prognostics

An essential part of the failure prognostics or RUL estimation is the degradation modeling since it is required to perform the projection of the state into future. To build such degradation models for prognosis purposes, researchers have tried to model the evolution/degradation of damage using physical degradation models such as applications in fatigue crack growth [39–41] and corrosion growth [6,7]. These physical degradation models are developed based on the understanding of the physical behavior and are usually validated by experiments. On the other hand, empirical degradation models are used when the evolution/degradation of damage is not well understood either due to limited understanding of the physical phenomenon or when the damage state cannot be measured continuously but rather occasionally. Approaches that combine physics-based approaches with data-driven methods have also been developed in recent years and lead to a group of hybrid approaches. A comprehensive review of prognostics approaches for rotating machine is available in [42].

For prognostics of civil infrastructure, however, the challenges come from the abstracted data sources and the lack of a degradation model. For example, the inspection

data are highly abstracted ratings as discussed in Sec. 2.2 and the ratings may be polluted by human errors as presented in Sec. 2.3. This section presents how to perform failure prognostics in this situation through three different approaches, namely

- Failure prognostics based on inspection data
- Failure prognostics using a continuous degradation model mapped from inspection data
- Integrated failure diagnostics and prognostics using dynamic Bayesian networks (DBN)

In the following subsections, the aforementioned three approaches are explained in detail.

4.1 Failure prognostics based on inspection data

As been discussed in Sec. 2.2, inspection data contains some degradation information of civil infrastructures even though they are highly abstracted. Since the damage state estimated from SHM is in continuous form, the continuous state can be converted into inspection data in discrete state through certain protocols. Taking the gap damage of a miter gate given in Fig. 2 as example, as shown in Fig. 12, the estimated gap length can be converted into gap state, which can then be used for failure prognostics using the gap state transition matrix given in Sec. 2.2.

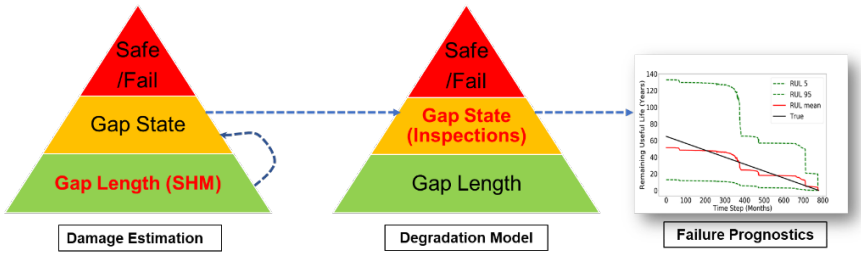

Fig. 12. Failure prognostics using inspection data.

More specifically, a certain protocol is usually needed to map the continuous damage state to the abstracted discrete state of inspection data. For instance, the gap length a_t of a miter gate (see Fig. 2) can be mapped into a gap state $X_{i,t}$ based on an engineering protocol as follows

$$R = h_{\mathrm{OCA}}(a_t, \boldsymbol{\beta}) = \begin{cases} X_{1,t} = A, a_t \in [0, \beta_1] \\ X_{2,t} = B, a_t \in [\beta_1, \beta_2] \\ X_{3,t} = C, a_t \in [\beta_2, \beta_3] \\ X_{4,t} = D, a_t \in [\beta_3, \beta_4] \\ X_{5,t} = F, a_t \in [\beta_4, \beta_5] \\ X_{6,t} = CF, a_t \in [\beta_5, \infty) \end{cases}, \tag{15}$$

where $\boldsymbol{\beta}=[\beta_1, \cdots, \beta_5]$ are protocol parameters defined by the field engineers.

Based on the mapping defined in the above equation, SHM data $\mathbf{s}_{1:n}$ can be used to estimate the gap state at current time step (i.e., highly abstracted inspection data) as follows

$$P(X_{i,n} \mid \mathbf{s}_{1:n}) = \Pr\left\{ X_n = X_{i,n} \mid \mathbf{s}_{1:n} \right\} = \begin{cases} \int_{\beta_{i-1}}^{\beta_i} f(a_n \mid \mathbf{s}_{1:n}) da_n, \text{if } i \le 5 \\ \int_{\beta_{i-1}}^{\infty} f(a_n \mid \mathbf{s}_{1:n}) da_n, \text{otherwise} \end{cases}, \forall i = 1, \cdots, 6, \tag{16}$$

where the PDF $f(a_n \mid \mathbf{s}_{1:n})$ of damage parameter a_n, is estimated using the Bayesian updating method presented in Sec. 3.2.

Once the gap state at current time step is estimated, the damage state of the failure *m* time steps into the future is obtained through the transition matrix given in Sec. 2.2 as

$$P\left(\mathbf{X}_{n+m} \mid \mathbf{s}_{1:n}\right) = P\left(\mathbf{X}_n \mid \mathbf{s}_{1:n}\right) \cdot \mathbf{P}_{\text{Report}}^m, \tag{17}$$

in which $\mathbf{P}_{\text{Report}}$ and $P\left(\mathbf{X}_n \mid \mathbf{s}_{1:n}\right)$ are respectively given in Eq. (1) and Eq. (16).

Using Eq. (17), the RUL for the system based on the current damage state and the future failure state can be estimated. Details on such predictions can be found in [23]. This approach assumes that the transition matrix $\mathbf{P}_{\text{Report}}$ can accurately represent the underlying degradation patten of the structure. However, this assumption is usually not true since the abstracted ratings are often biased by human errors as discussed in Sec. 2.3. To tackle this issue, an approach has been proposed in [10] to map the reported transition matrix to a more useful transition matrix that has eliminated some of the effects of the human errors. In order to map the reported rating transition matrix $\mathbf{P}_{\text{Report}}$ to the underlying "true" transition matrix $\mathbf{P}_{\text{True}}$, the underlying true transition rating is defined at time *t* as X_t^{tr} and that at *t*+1 as X_{t+1}^{tr}. Similarly, the reported ratings from field engineers are defined at time *t* as X_t^{obs} and that at time *t*+1 as X_{t+1}^{obs}. Based on these definitions and using the human error matrix given in Eq. (3), $\mathbf{P}_{\text{Report}}$ can then be mapped into $\mathbf{P}_{\text{True}}$ by following the procedure shown in Fig. 13. More details of Fig. 13 are available in [1]. Once $\mathbf{P}_{\text{True}}$ is obtained, it can be used to substitute $\mathbf{P}_{\text{Report}}$ in Eq. (17) to get more accurate failure prognostics results.

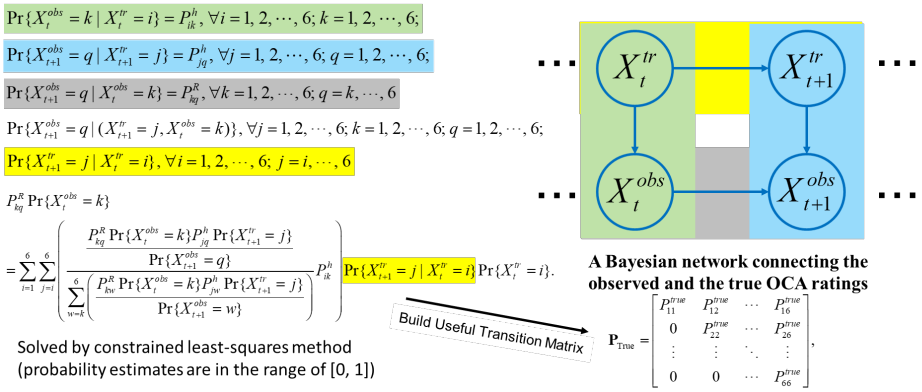

Fig. 13. Mapping between reported transition matrix to compensated/true transition matrix

In addition, a Bayesian method has also been developed in [23] to update the errors in the transition matrix using SHM data. The advantage of the approach presented here is that it requires minimal information for failure prognostics. The disadvantage is that there is very large uncertainty in the obtained RUL estimation results. Alternatively, a stochastic continuous degradation model can be built to improve the confidence of such predictions of the damage parameters which leads to better failure prognostics.

4.2 Mapping inspection data into continuous degradation model for failure prognostics

Using the gap growth of miter gate as an example, as shown in Fig. 14, an alternative approach to perform failure prognostics is to map the abstracted inspection data into a degradation model in continuous space and then perform failure prognostics in the continuous space. It is expected that prognostics in continuous space can increase the confidence of RUL estimation.

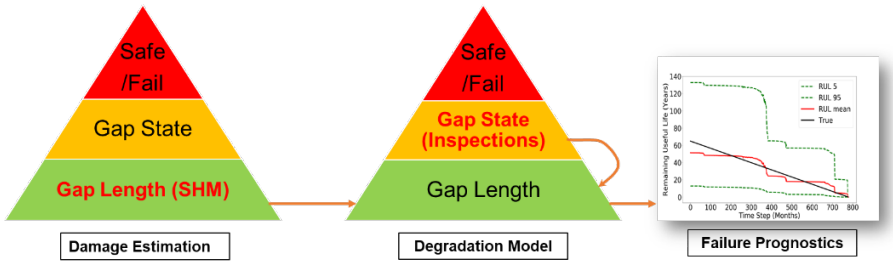

Fig. 14. Failure prognostics in continuous space by mapping inspection data into a degradation model.

For a transition matrix $\mathbf{P}_{\text{Report}}$ given in Section 2.2 or $\mathbf{P}_{\text{True}}$ obtained in Sec. 4.1 after mitigating human error bias, a continuous degradation model can be obtained through Bayesian or optimization-based calibration. More details of the mapping from inspection data to a degradation model are available in [10]. Here, a brief summary of the

major steps is presented. When optimization-based method is employed, the optimization model is given by

$$g_{opt}(\boldsymbol{\theta};\mathbf{P}_{\text{True}}) = \left\| \hat{\mathbf{P}}(\boldsymbol{\theta}) - \mathbf{P}_{\text{True}} \right\|_2, \tag{18}$$

where $\hat{\mathbf{P}}(\boldsymbol{\theta})$ is the simulated transition matrix for a given degradation model with parameters $\boldsymbol{\theta}$.

The most critical part is how to estimate $\boldsymbol{\theta}$ for given $\mathbf{P}_{\text{True}}$. To do that, $\hat{\mathbf{P}}(\boldsymbol{\theta})$ is calibrated for any given $\boldsymbol{\theta}$. The degradation model is modelled as a multi-stage degradation model as follows

$$\frac{da(t)}{dt} = \exp(\sigma_j(t)U(t))Q_j(t)(a(t))^{w_j(t)}, \forall j = 1, \cdots, N_d, \tag{19}$$

where $a(t)$ is the gap length at time *t*, Q_i and w_i are stage-dependent degradation parameters, σ_i is a standard deviation variable of degradation stage *i*, and $U(t)$ is a stationary standard Gaussian process with auto-correlation function given by

$$cov(U(t_1), U(t_2)) = \exp(-\zeta|t_2 - t_1|), \tag{20}$$

in which ζ is a correlation length parameter.

For the above degradation model and given degradation model parameters, a large number of realizations of the degradation curves is simulated using the Monte Carlo simulation method. The obtained realizations of the degradation curves in the continuous space can then be converted into ratings in the discrete states as follows

$$X_n = X_{stage}(a_n) = \begin{cases} X_{1,n}, & a_n \in [e_0, e_1) \\ X_{2,n}, & a_n \in [e_1, e_2) \\ X_{3,n}, & a_n \in [e_2, e_3) \\ X_{4,n}, & a_n \in [e_3, e_4) \\ X_{5,n}, & a_n \in [e_4, e_5) \\ X_{6,n}, & a_n \geq e_5 \end{cases}, \tag{21}$$

where $e_j, \forall j = 1, \cdots, 5$ are parameters that govern the transition between different stages of degradations in the continuous space.

After the simulated degradation curves are converted into degradation ratings using Eq. (21), the simulated transition matrix $\hat{\mathbf{P}}(\boldsymbol{\theta})$ can be obtained. For the above degradation model, the parameters of the degradation model, $\boldsymbol{\theta}$, can therefored be summarized as follows

$$\begin{aligned} &\boldsymbol{\theta} \triangleq (\boldsymbol{\theta}_1, \boldsymbol{\theta}_2, \boldsymbol{\theta}_3, \boldsymbol{\theta}_4, \boldsymbol{\theta}_5, e_1, e_2, e_3, e_4, \sigma), \text{ where} \\ &\boldsymbol{\theta}_{\mathbf{j}} \triangleq \{\sigma_j, \zeta_j, Q_j, w_j, \text{ j} = 1,2,....5\}. \end{aligned} \tag{22}$$

Then, the degradation model can be estimated as follows using the optimization model given in Eq. (18). Fig. 15 summarizes the overall procedure of estimating $\hat{\mathbf{P}}(\boldsymbol{\theta})$ for a given degradation model and model parameters $\boldsymbol{\theta}$.

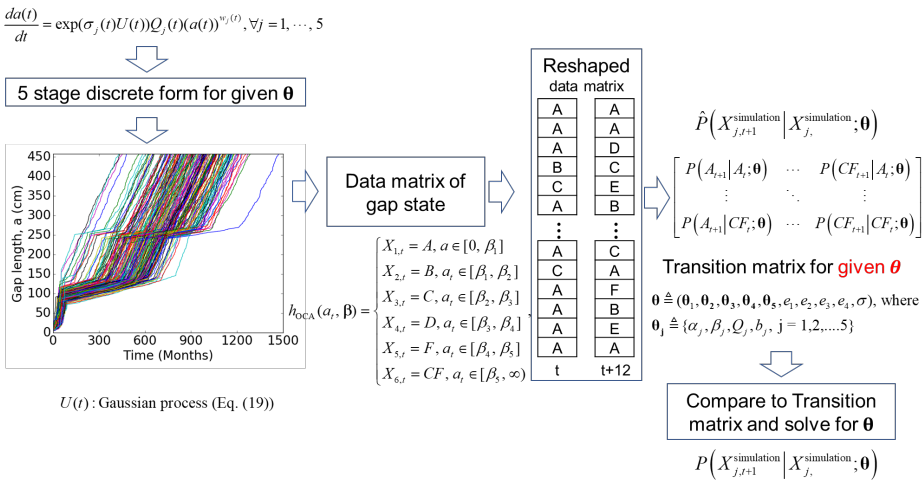

Fig. 15. Overview of obtaining simulated transition matrix for given $\boldsymbol{\theta}$.

Once the degradation model is available, it can be used for failure prognostics in the continuous space as illustrated in Fig. 11. This procedure, however, is not limited to the model given in Eq. (19). It is also applicable to other degradation models and can be integrated into a Bayesian framework. More detailed discussions of this approach can be found in [10].

Fig. 16 depicts a comparison of the RUL estimates obtained using the approaches presented in Sec. 4.1 (denoted as TM mean prediction, TM Conf. limit) and Sec. 4.2, respectively. It shows that mapping inspection data into a continuous degradation model can significantly increase the confidence of the failure prognostics results.

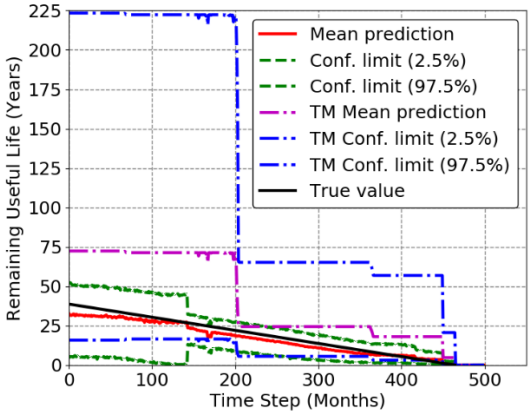

Fig. 16. Comparison of RUL estimates using discrete degradation model (Sec. 4.1) and piece-wise continuous degradation model (Sec. 4.2).

4.3 Integrated failure diagnostics and prognostics using dynamic Bayesian networks

Failure diagnostics and prognostics of civil infrastructure usually require the usage of multiple models including degradation model [39–41] and physics-based model [12–14], as discussed earlier. In addition to various analysis models, heterogeneous data and uncertainty sources are involved in the process of diagnostics and prognostics. A flexible tool that can be used to tackle the challenges in diagnostics and prognostics caused by the heterogeneity of model and data sources is Bayesian networks (BN).

A BN, which is also called probabilistic graphic model, is a directed acyclic graph that connects different variables in a probabilistic way. It allows for the flexible integration of multi-type of models and information sources in a systematic Bayesian framework, and thereby enable decision makers to update information and reduce uncertainty in a holistic manner [43]. Due to its capability of fusing information and data sources, BN plays a vital role in building digital twins for SHM in various assets, from aerospace engineering to civil and mechanical engineering [40,44].

For n random variables (nodes), $X_1, X_2, \cdots,$ and X_n, BN represents the joint probability density function $p(\mathbf{X})$ as follows

$$p(\mathbf{X}) = p(X_1, X_2, \cdots, X_n) = \prod_{i=1}^{n} p(X_i \mid \boldsymbol{\pi}_i), \tag{23}$$

where $\boldsymbol{\pi}_i$ is a set of parent nodes of X_i, $p(X_i \mid \boldsymbol{\pi}_i)$ is the conditional probability mass (CPM) function or conditional probability density (CPD) function, and nodes without parent nodes are called root nodes. For root nodes, assume $p(X_i \mid \boldsymbol{\pi}_i) = p(X_i)$.

A type of widely used BN in failure diagnostics and prognostics is the dynamic Bayesian network (DBN). Fig. 17 shows a simple example of DBN. As shown in this figure, the DBN consists of state variable denoted by a_t and measurement variable represented by $\mathbf{s}_t$. The CPD function $f(a_t \mid a_{t-1})$ describes the transition of the state variable a_t over time and $h(\mathbf{s}_{t-1} \mid a_{t-1})$ models the probabilistic relationship between the state variable and measurement variable. When the state variables are variables related to the failure modes or degradation stages of the civil infrastructure, the measurements collected from measurement variable $\mathbf{s}_t$ can be used for failure diagnostics using Bayesian inference methods. Based on the failure diagnostics or estimation of damage related state variables, failure prognostics may then be performed according the transition of state variables over time, which is governed by the CPD function $f(a_t \mid a_{t-1})$.

In practical engineering applications, the node in the DBN can be a mathematical model, a finite element model, or a data-driven machine learning model. The DBN used for failure diagnostics and prognostics can be constructed using physics-based method [12–14], Bayesian network learning method [44], or a hybrid of physics and data-driven methods [19,20].

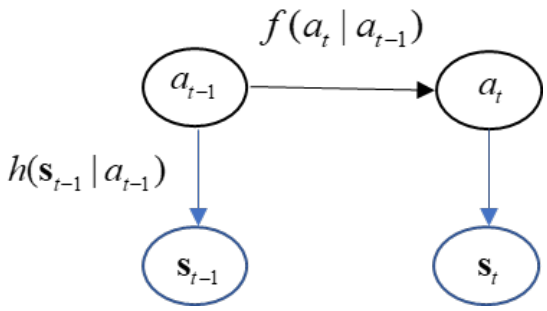

Fig. 17. An example of dynamic Bayesian network

Fig. 18 depicts a schematic Dynamic Bayesian network at one time instant for the failure diagnostics and prognostics of a miter gate (see Fig. 2), which is used an example to explain the presented approaches in this chapter. Note that, for the sake of simplification, the transient BN is not depicted. As shown in this figure, the DBN connects variables of a degradation model with variables of a strain analysis model of the miter gate. For example, the parent nodes of node e_1 in Fig. 18 are nodes σ_e and μ_1. The CPDs in the DBN can be derived according to the approaches discussed in Sec. 3.2 and Sec. 4.2 of this chapter. Using the strain measurement collected from SHM system, the uncertain variables of the degradation model can be updated. The updated degradation model can then be used to estimate RUL of the gate dynamically over time.

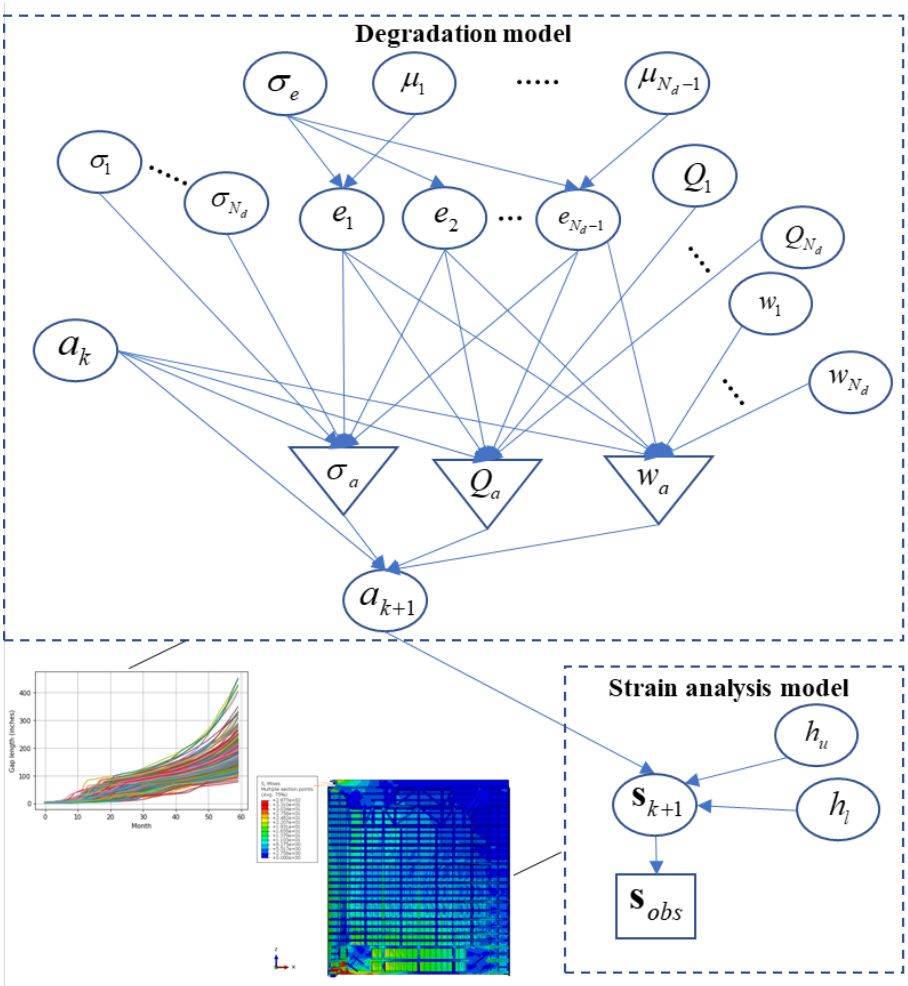

Fig. 18. A schematic Bayesian network of a miter gate at one time instant for diagnostics and prognostics.

Fig. 19 presents an illustrative example of the posterior distribution updating of parameter w_1 over time using the strain measurements of the miter gate. Following that, Fig. 20 depicts the RUL estimation of the miter gate over time. It shows that the confidence of RUL estimation increases over time as more and more measurements are collected. Additionally, it is worth mentioning that the degradation model and strain analysis model are updated in an integrated manner in the DBN-based framework. This example illustrates the flexibility of DBN in connecting multiple models for failure diagnostics and prognostics. A good application of DBN for the failure diagnostics and prognostics is available in [45].

Moreover, the degradation model parameters obtained in Sec. 4.2 using optimization or Bayesian-based method can be used as prior information for the DBN-based method.

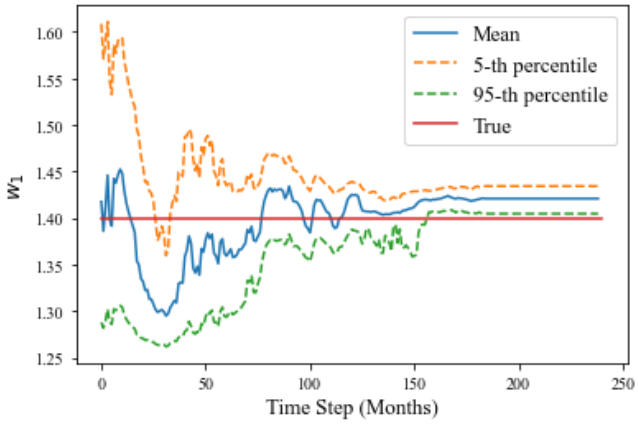

Fig. 19. An illustrative example of updating posterior distribution of a degradation model parameter using DBN over time.

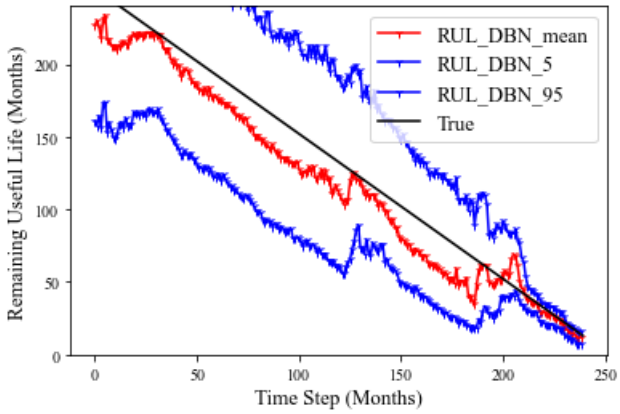

Fig. 20. RUL estimation over time of the miter gate.

In summary, this section presents three different approaches for failure diagnostics using Bayesian data analytics and machine learning. The advantage of the approach presented in Sec. 4.1 requires minimal information for failure prognostics. The advantages of the approaches presented in Secs. 4.2 and 4.3 are that they can provide prediction results with less uncertainty. Next, the maintenance planning based on failure diagnostics and prognostics is briefly introduced.

5 Optimization of maintenance strategy

As mentioned in Sec. 1, there are two types of maintenance strategies, namely TBM and CBM. TBM (also known as periodic-based maintenance) assumes that the estimated failure behavior is statistically or experientially known [46]. Statistical modelling, such as Weibull analysis [47], is widely used in TBM to identify failure characteristics of a component or system. The goal of TBM models is to find the optimal

policy that minimize a cost function. TBM approaches have been developed for both repairable or nonrepairable systems [48]. The complexity of a TBM model depends on the targeted system such as single-system, multi-systems, parallel and series structure. A more extensive review of TBM applications can be found here [49]. For example, in miter gates, historical data is available in the form of discrete ratings

Fig. 21 shows a TBM approach using the transition matrix given in Sec. 2.2, whose goal is to estimate the optimal maintenance time based on a well-known cost function [48], which weight the probability of failure, $F(t)$, with the preventive, C_p, and unscheduled (or emergency), C_u, maintenance costs,

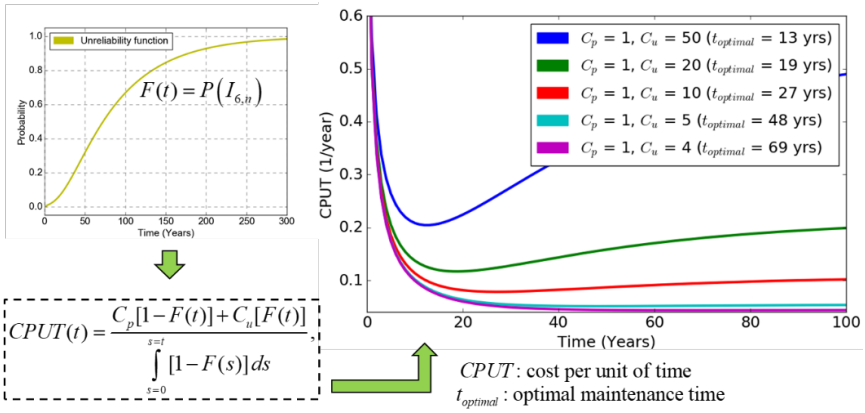

Fig. 21. TBM approach using discrete ratings

CBM is the most modern and popular maintenance technique among researchers and industry. CBM has gained increasing attention recently as a preferred approach to TBM. CBM is a maintenance approach that combines data-driven reliability models and information from a condition monitoring process. Based on the underlying degradation model, CBM models can be categorized into two subgroups: 1) models that assume discrete-state deterioration (such as in Sec. 4.1) and 2) models that assume continuous state deterioration (such as in Secs. 4.2 and 4.3). A most extensive list of CBM application can be found in here [50–53]. Most of the CBM applications available in the literature are for mechanical systems, aerospace systems, or manufacturing systems. For large civil engineering infrastructure, most of the applications have been applied to bridge engineering [54–56]. In CBM, maintenance schedules are predicted based on the results from diagnosis and prognosis, as discussed in Secs. 3 and 4. For diagnosis and prognosis, CBM approaches can be classified into physics-based approach [12–14], data-driven approach [15–18], and hybrid approach [19,20]. The approaches presented in this book chapter can be classified as hybrid approaches since they combine physics-based approach with data-driven approach to improve CBM predictive capabilities.

6 Conclusion

This chapter presents comprehensive failure diagnostics, prognostics, and maintenance planning approaches using machine learning, Bayesian data analysis, computational mechanics, and reliability engineering. The presented framework is aimed to allow real-time assessments of civil structures that has different forms of available data. The challenge of heterogeneity of the data sources has been successfully overcome to provide diagnostic/prognostic capabilities to the structure of interest. Additional steps have been discussed to improve these capabilities such as optimal sensor design and accounting for human error. Currently, the features used to update the models used in this work have been based on SHM data and human inspections. However, this framework can be adapted to work with more advanced data sources enhanced with supervised learning algorithms such images captured from drones or robots.

7 References

[1] Vega MA. Diagnosis, Prognosis, and Maintenance Decision Making for Civil Infrastructuree. UC San Diego, 2020.

[2] Moaveni B, Conte JP, Hemez FM. Uncertainty and Sensitivity Analysis of Damage Identification Results Obtained Using Finite Element Model Updating. Comput Civ Infrastruct Eng 2009;24:320–34. https://doi.org/10.1111/j.1467-8667.2008.00589.x.

[3] Jang S, Li J, Spencer BF. Corrosion Estimation of a Historic Truss Bridge Using Model Updating. J Bridg Eng 2013;18:678–89. https://doi.org/10.1061/(ASCE)BE.1943-5592.0000403.

[4] Vega MA, Ramancha MR, Conte JP, Todd MD. Efficient Bayesian Inference of Miter Gates using High-Fidelity Models. 38th Int. Modal Anal. Conf., Houston, Texas: Springer; 2020.

[5] Kim N-H, An D, Choi J-H. Prognostics and Health Management of Engineering Systems. Cham: Springer International Publishing; 2017. https://doi.org/10.1007/978-3-319-44742-1.

[6] Guedes Soares C, Garbatov Y, Zayed A. Effect of environmental factors on steel plate corrosion under marine immersion conditions. Corros Eng Sci Technol 2011;46:524–41. https://doi.org/10.1179/147842209X12559428167841.

[7] Wang C, Elsayed EA. Stochastic modeling of corrosion growth. Reliab Eng Syst Saf 2020;204:107120. https://doi.org/10.1016/j.ress.2020.107120.

[8] Si X-S, Wang W, Hu C-H, Zhou D-H. Remaining useful life estimation – A review on the statistical data driven approaches. Eur J Oper Res 2011;213:1–14. https://doi.org/10.1016/j.ejor.2010.11.018.

[9] Wang Z, Shafieezadeh A. Real-time high-fidelity reliability updating with equality information using adaptive Kriging. Reliab Eng Syst Saf 2020;195:106735. https://doi.org/10.1016/j.ress.2019.106735.

[10] Vega M, Hu Z, Fillmore T, Smith M, Todd M. A Novel Framework for Integration of Abstracted Inspection Data and Structural Health Monitoring for Gap Prognosis of Miter Gates (Under Review). Reliab Eng Syst Saf n.d.

[11] Mitchell JS. From vibration measurements to condition based maintenance seventy

years of continuous progress. Sound Vib 2007;41:62–78.
[12] Orchard ME, Vachtsevanos GJ. A Particle Filtering Approach for On-Line Failure Prognosis in a Planetary Carrier Plate. Int J Fuzzy Log Intell Syst 2007;7:221–7. https://doi.org/10.5391/IJFIS.2007.7.4.221.
[13] Daigle M, Goebel K. Multiple damage progression paths in model-based prognostics. 2011 Aerosp. Conf., IEEE; 2011, p. 1–10. https://doi.org/10.1109/AERO.2011.5747574.
[14] An D, Choi J-H, Schmitz TL, Kim NH. In situ monitoring and prediction of progressive joint wear using Bayesian statistics. Wear 2011;270:828–38. https://doi.org/10.1016/j.wear.2011.02.010.
[15] Zio E, Di Maio F. A data-driven fuzzy approach for predicting the remaining useful life in dynamic failure scenarios of a nuclear system. Reliab Eng Syst Saf 2010;95:49–57. https://doi.org/10.1016/j.ress.2009.08.001.
[16] Mohanty S, Das S, Chattopadhyay A, Peralta P. Gaussian Process Time Series Model for Life Prognosis of Metallic Structures. J Intell Mater Syst Struct 2009;20:887–96. https://doi.org/10.1177/1045389X08099602.
[17] Galar D, Kumar U, Lee J, Zhao W. Remaining Useful Life Estimation using Time Trajectory Tracking and Support Vector Machines. J Phys Conf Ser 2012;364:012063. https://doi.org/10.1088/1742-6596/364/1/012063.
[18] Ye Z-S, Xie M. Stochastic modelling and analysis of degradation for highly reliable products. Appl Stoch Model Bus Ind 2015;31:16–32. https://doi.org/10.1002/asmb.2063.
[19] Xu J, Xu L. Health management based on fusion prognostics for avionics systems. J Syst Eng Electron 2011;22:428–36. https://doi.org/10.3969/j.issn.1004-4132.2011.03.010.
[20] Liao L, Kottig F. Review of Hybrid Prognostics Approaches for Remaining Useful Life Prediction of Engineered Systems, and an Application to Battery Life Prediction. IEEE Trans Reliab 2014;63:191–207. https://doi.org/10.1109/TR.2014.2299152.
[21] Spencer BF, Hoskere V, Narazaki Y. Advances in Computer Vision-Based Civil Infrastructure Inspection and Monitoring. Engineering 2019;5:199–222. https://doi.org/10.1016/j.eng.2018.11.030.
[22] Gibb S, La HM, Le T, Nguyen L, Schmid R, Pham H. Nondestructive evaluation sensor fusion with autonomous robotic system for civil infrastructure inspection. J F Robot 2018;35:988–1004. https://doi.org/10.1002/rob.21791.
[23] Vega MA, Hu Z, Todd MD. Optimal maintenance decisions for deteriorating quoin blocks in miter gates subject to uncertainty in the condition rating protocol. Reliab Eng Syst Saf 2020;204:107147. https://doi.org/10.1016/j.ress.2020.107147.
[24] Campbell LE, Connor RJ, Whitehead JM, Washer GA. Benchmark for Evaluating Performance in Visual Inspection of Fatigue Cracking in Steel Bridges. J Bridg Eng 2020;25:04019128. https://doi.org/10.1061/(ASCE)BE.1943-5592.0001507.
[25] Yin T, Zhu H. Probabilistic Damage Detection of a Steel Truss Bridge Model by Optimally Designed Bayesian Neural Network. Sensors 2018;18:3371. https://doi.org/10.3390/s18103371.
[26] Chua CG, Goh ATC. Estimating wall deflections in deep excavations using Bayesian neural networks. Tunn Undergr Sp Technol 2005;20:400–9.

https://doi.org/10.1016/j.tust.2005.02.001.
[27] Arangio S, Bontempi F. Structural health monitoring of a cable-stayed bridge with Bayesian neural networks. Struct Infrastruct Eng 2015;11:575–87. https://doi.org/10.1080/15732479.2014.951867.
[28] Vega MA, Todd MD. A variational Bayesian neural network for structural health monitoring and cost-informed decision-making in miter gates. Struct Heal Monit 2020. https://doi.org/10.1177/1475921720904543.
[29] Parno M, O'Connor D, Smith M. High dimensional inference for the structural health monitoring of lock gates 2018:1–29.
[30] Doucet A, Freitas N de, Gordon N. Sequential Monte Carlo Methods in Practice. New York, NY: Springer New York; 2001. https://doi.org/10.1007/978-1-4757-3437-9.
[31] Mochnac J, Marchevsky S, Kocan P. Bayesian filtering techniques: Kalman and extended Kalman filter basics. 2009 19th Int. Conf. Radioelektronika, IEEE; 2009, p. 119–22. https://doi.org/10.1109/RADIOELEK.2009.5158765.
[32] Julier SJ, Uhlmann JK. Unscented Filtering and Nonlinear Estimation. Proc IEEE 2004;92:401–22. https://doi.org/10.1109/JPROC.2003.823141.
[33] Tenney R, Sandell N. Detection with Distributed Sensors. IEEE Trans Aerosp Electron Syst 1981;AES-17:501–10. https://doi.org/10.1109/TAES.1981.309178.
[34] Flynn EB, Todd MD. A Bayesian approach to optimal sensor placement for structural health monitoring with application to active sensing. Mech Syst Signal Process 2010;24:891–903. https://doi.org/10.1016/j.ymssp.2009.09.003.
[35] Nath P, Hu Z, Mahadevan S. Sensor placement for calibration of spatially varying model parameters. J Comput Phys 2017;343:150–69. https://doi.org/10.1016/j.jcp.2017.04.033.
[36] Jones DR, Schonlau M, Welch WJ. Efficient Global Optimization of Expensive Black-Box Functions. J Glob Optim 1998;13:455–92.
[37] Hu Z, Du X. Mixed Efficient Global Optimization for Time-Dependent Reliability Analysis. J Mech Des 2015;137. https://doi.org/10.1115/1.4029520.
[38] Yang Y, Chadha M, Hu Z, Parno M, Vega M, Todd MD. A Probabilistic Optimal Sensor Design Approach for Structural Health Monitoring Using Risk-Weighted f-Divergence (Under Review). Mech Syst Signal Process 2021.
[39] An D, Choi J-H, Kim NH. Identification of correlated damage parameters under noise and bias using Bayesian inference. Struct Heal Monit An Int J 2012;11:293–303. https://doi.org/10.1177/1475921711424520.
[40] Li C, Mahadevan S, Ling Y, Choze S, Wang L. Dynamic Bayesian Network for Aircraft Wing Health Monitoring Digital Twin. AIAA J 2017;55:930–41. https://doi.org/10.2514/1.J055201.
[41] Leung MSH, Corcoran J, Cawley P, Todd MD. Evaluating the use of rate-based monitoring for improved fatigue remnant life predictions. Int J Fatigue 2019;120:162–74. https://doi.org/10.1016/j.ijfatigue.2018.11.012.
[42] Cubillo A, Perinpanayagam S, Esperon-Miguez M. A review of physics-based models in prognostics: Application to gears and bearings of rotating machinery. Adv Mech Eng 2016;8:168781401666466. https://doi.org/10.1177/1687814016664660.
[43] Sankararaman S, Ling Y, Mahadevan S. Uncertainty quantification and model validation of fatigue crack growth prediction. Eng Fract Mech 2011;78:1487–504.

https://doi.org/10.1016/j.engfracmech.2011.02.017.
[44] Hu Z, Mahadevan S. Bayesian Network Learning for Data-Driven Design. ASCE-ASME J Risk Uncert Engrg Sys Part B Mech Engrg 2018;4:1–12. https://doi.org/10.1115/1.4039149.
[45] Rafiq MI, Chryssanthopoulos MK, Sathananthan S. Bridge condition modelling and prediction using dynamic Bayesian belief networks. Struct Infrastruct Eng 2015;11:38–50. https://doi.org/10.1080/15732479.2013.879319.
[46] Yam RCM, Tse PW, Li L, Tu P. Intelligent Predictive Decision Support System for Condition-Based Maintenance. Int J Adv Manuf Technol 2001;17:383–91. https://doi.org/10.1007/s001700170173.
[47] Weibull W. A Statistical Distribution Function of Wide Applicability. J Appl Mech 1951;103:293–7.
[48] Barlow R, Hunter L. Optimum Preventive Maintenance Policies. Oper Res 1960;8:90–100. https://doi.org/10.1287/opre.8.1.90.
[49] Ahmad R, Kamaruddin S. An overview of time-based and condition-based maintenance in industrial application. Comput Ind Eng 2012;63:135–49. https://doi.org/10.1016/j.cie.2012.02.002.
[50] Zhu Y, Elsayed EA, Liao H, Chan LY. Availability optimization of systems subject to competing risk. Eur J Oper Res 2010;202:781–8. https://doi.org/10.1016/j.ejor.2009.06.008.
[51] Tian Z, Jin T, Wu B, Ding F. Condition based maintenance optimization for wind power generation systems under continuous monitoring. Renew Energy 2011;36:1502–9. https://doi.org/10.1016/j.renene.2010.10.028.
[52] Tian Z, Liao H. Condition based maintenance optimization for multi-component systems using proportional hazards model. Reliab Eng Syst Saf 2011;96:581–9. https://doi.org/10.1016/j.ress.2010.12.023.
[53] Alaswad S, Xiang Y. A review on condition-based maintenance optimization models for stochastically deteriorating system. Reliab Eng Syst Saf 2017;157:54–63. https://doi.org/10.1016/j.ress.2016.08.009.
[54] Petcherdchoo A, Neves LA, Frangopol DM. Optimizing Lifetime Condition and Reliability of Deteriorating Structures with Emphasis on Bridges. J Struct Eng 2008;134:544–52. https://doi.org/10.1061/(ASCE)0733-9445(2008)134:4(544).
[55] Saydam D, Frangopol DM. Risk-Based Maintenance Optimization of Deteriorating Bridges. J Struct Eng 2015;141:04014120. https://doi.org/10.1061/(ASCE)ST.1943-541X.0001038.
[56] Gong C, Frangopol DM. Condition-Based Multiobjective Maintenance Decision Making for Highway Bridges Considering Risk Perceptions. J Struct Eng 2020;146:04020051. https://doi.org/10.1061/(ASCE)ST.1943-541X.0002570.